PL-TR-93-2001

MODERN SEISMIC TRAVEL TIME TABLES AND STATION CORRECTIONS FOR P AND S WAVES

John A. Orcutt

University of California, San Diego
Scripps Institution of Oceanography
La Jolla, CA 92093

13 December 1992

Final Report
13 September 1990 - 13 December 1992

PHILLIPS LABORATORY
Directorate of Geophysics
AIR FORCE MATERIEL COMMAND
HANSCOM AIR FORCE BASE, MA 01731-5000

SPONSORED BY
Defense Advanced Research Projects Agency
Nuclear Monitoring Research Office, and
Defense Sciences Office
ARPA ORDER NO 5299

MONITORED BY
Phillips Laboratory
CONTRACT NO. F19628-90-K-0053

This technical report has been reviewed and is approved for publication.

JAMES F. LEWKOWICZ
Contract Manager
Solid Earth Geophysics Branch
Earth Sciences Division

JAMES F. LEWKOWICZ
Branch Chief
Solid Earth Geophysics Branch
Earth Sciences Division

DONALD H. ECKHARDT, Director
Earth Sciences Division

This report has been reviewed by the ESD Public Affairs Office (PA) and is releasable to the National Technical Information Service (NTIS).

Qualified requestors may obtain additional copies from the Defense Technical Information Center. All others should apply to the National Technical Information Service.

If your address has changed, or if you wish to be removed from the mailing list, or if the addressee is no longer employed by your organization, please notify GL/IMA, Hanscom AFB, MA 01731-5000. This will assist us in maintaining a current mailing list.

Do not return copies of this report unless contractual obligations or notices on a specific document requires that it be returned.

REPORT DOCUMENTATION PAGE

Form Approved
OMB No 0704-0188

1. AGENCY USE ONLY (Leave blank)	2. REPORT DATE	3. REPORT TYPE AND DATES COVERED
	13 December 1992	Final (13 Sep 1990-13 Dec 1992)

4. TITLE AND SUBTITLE
Modern seismic travel time tables and station corrections for P and S waves

5. FUNDING NUMBERS
PE 61101E
PR 0A10-TA DA - WU AF
Contract F19628-90-K-0053

6. AUTHOR(S)
John A. Orcutt

7. PERFORMING ORGANIZATION NAME(S) AND ADDRESS(ES)
University of California, San Diego
Scripps Institution of Oceanography
La Jolla, CA 92093

8. PERFORMING ORGANIZATION REPORT NUMBER

9. SPONSORING/MONITORING AGENCY NAME(S) AND ADDRESS(ES)
Phillips Laboratory
Hanscom AFB, MA 01731-5000

Contract manager: James Lewkowicz/GPEH

10. SPONSORING/MONITORING AGENCY REPORT NUMBER
PL-TR-93-2001

11. SUPPLEMENTARY NOTES

12a. DISTRIBUTION/AVAILABILITY STATEMENT
Approved for public release;
distribution unlimited.

12b. DISTRIBUTION CODE

13. ABSTRACT (Maximum 200 words)

1) We refine estimates of inner core structure by examining PKP travel times and find that anisotropy is a simpler explanation than heterogeneity for the observed residual patterns. Our preferred model of inner core anisotropy contains velocities that are 0.5% faster in a N-S direction than an E-W direction. 2) We study various mantle differential travel times including SS-S, ScS-S, PP-P, and PcP-P and compare these results to those obtained from handpicked waveform data. Large-scale coherent patterns of residuals are seen which indicate mantle heterogeneity. 3) We examine PKP travel times to study the possibility of outer core heterogeneity models which are suggested by observations of anomalous splitting in normal modes. We find that the travel times limit the scale of possible outer core heterogeneity to models much smaller than those required to explain the mode splitting data. 4) We develop computer codes which return travel time and ray geometries for a given seismic phase, source-receiver pair, and arbitrary 3-d earth models specified by their spherical harmonic expansions.

14. SUBJECT TERMS	15. NUMBER OF PAGES
Seismic travel times, Earth models, core structure	36
	16. PRICE CODE

17. SECURITY CLASSIFICATION OF REPORT	18. SECURITY CLASSIFICATION OF THIS PAGE	19. SECURITY CLASSIFICATION OF ABSTRACT	20. LIMITATION OF ABSTRACT
Unclassified	Unclassified	Unclassified	SAR

TASK OBJECTIVES

The broad objective of this research is to understand the mapping of seismic travel time data into the Earth's velocity structure. We are developing a self-consistent set of mantle and core velocity models and station corrections, utilizing all the available phase data in the ISC catalog. These models will provide AFOSR and AFTAC with a self-consistent Earth model for use in generating travel times for phase identification and event location.

Specifically, the work statement includes the following:

- Extension of radial model work to core and other mantle phases
  - Core phases *PKP*, *SKS*, and *PKIKP*
  - Better mantle *S* wave model from core phases
  - Multiple phases, such as *pP*, *sS*, *PP* and *SS*
  - Better control on source depth from depth phases
  - *PP* and *SS* residual patterns to find bouncepoint "correction"
  - Core reflected phases *PcP* and *ScS*
  - Inversion of all ISC phase data for improved radial earth model
- Computer program for travel time curves
  - Program to give ray geometry for given source-receiver pair
  - Distribute program on various media for general use

TECHNICAL RESULTS

ABSTRACT

In this report we present the results of several investigations dealing with different topics:

- We refine estimates of inner core structure by examining differential *PKP* travel times and find that anisotropy is a simpler explanation than heterogeneity for the observed residual patterns. Our preferred model of inner core anisotropy contains velocities that are 0.5% faster in a N-S direction that an E-W direction.

- We study various mantle differential travel times including *SS–S*, *ScS–S*, *PP–P*, and *PcP–P* and compare these results to those obtained from handpicked waveform data. Large-scale coherent patterns of residuals are seen which indicate mantle heterogeneity.

- We examine *PKP* travel times to study the possibility of outer core heterogeneity models which are suggested by observations of anomalous splitting in normal modes. We find that the travel times limit the scale of possible outer core heterogeneity to models much smaller than those required to explain the mode splitting data.

• We develop computer codes which return travel time and ray geometries for a given seismic phase, source-receiver pair, and arbitrary 3-d earth models specified by their spherical harmonic expansions.

PART 1: INNER CORE STRUCTURE

We have estimated inner core anisotropy by examining differential *PKP* travel times. *PKP(BC)* versus *PKP(DF)* travel times show coherent patterns of residuals indicating aspherical structure within the Earth's inner core. Figure 1 shows 19,470 probable *BC* versus *DF* travel times at ranges between 145° and 155° obtained from 23 years of the ISC catalog. These times were obtained by finding the difference between any pairs of picks within a time window around the predicted *PKP* arrival times. The diagonal banding results from the 0.1 s resolution of the ISC picks and the tendency for operators to pick even seconds or half seconds. A hint of the *AB* branch can be seen sloping away near 148° range. Using a bin averaging scheme in which points on a sphere are combined within 416 approximately equal area cells we produced plots of average residual versus turning point position (Figure 2) and versus ray direction (Figure 3). Positive residuals are indicated with crosses and negative residuals with diamonds; the size of the symbol indicates the magnitude of the residual. The turning point position plot is most sensitive to inner core heterogeneity, while the ray angle plot is most sensitive to inner core anisotropy. Large positive residuals are seen near the poles in the ray-direction plot, indicating fast N-S inner core velocities. This result is in agreement with previous studies of absolute *PKP* residuals but derived from an independent data set. Due to the sparse ray coverage of our data, either heterogeneity of anisotropy within the inner core with about 1% velocity variations could explain the residual patterns seen in Figures 2 and 3. However, inversions of the ISC data for heterogeneity require many more free parameters to achieve the same variance reduction as a simple 2 parameter anisotropy model.

Shearer, P.M., and K.M. Toy, 1991, PKP(BC) versus PKP(DF) differential travel times and aspherical structure in the Earth's inner core, *J. Geophys. Res.*, 96, 2233-2247.

PART 2: DIFFERENTIAL TRAVEL TIMES

We copied the ISC travel times into a condensed binary format which provides on-line access to the data from our HP/Apollo computer network. We have extracted *PP-P*, *SS-S*, *PcP-P*, and *ScS-S* differential travel times for further analysis and comparisons with results obtained for long-period data. The ISC data base from 1964 to 1987 currently contains over 9 million global travel times (Figure 4). By separating earthquake and station information and storing the data in binary (rather than ASCII), we have reduced the storage requirements of this data set to about 100 Mbytes, or slightly over 10 bytes per travel time. A data base of this size can be left on magnetic disk for convenient access. In addition, the use of binary block read and write statements means that the entire data set can be retrieved and stored in a matter of several minutes.

We have examined differential travel time pairs in the ISC data. Differential times have many advantages in travel time analyses since they are relatively insensitive to errors in earthquake depths and origin times. Figure 5 shows the results of extracting all pairs of

arrivals at a single station in which one of the arrivals was within 20 s of the predicted *S*-wave travel time. Each point plotted is a differential time relative to the *S*-wave pick shown at zero time. Only shallow events (< 50 km) deep are shown to avoid complications due to depth phases. Many additional phases are apparent in this plot, including *PcS*, *ScS*, *SKS*, *PS*, *PPS*, *SS*, and *SSS*. We extracted 25,419 *SS - S* differential times and 20,821 *ScS - S* times from picks tabulated by the ISC from 1964 to 1987. This was done by identifying pairs of picks from a station for a particular event, where each pick is within 20 s of the predicted arrival time. These differential times exhibit much less scatter than absolute ISC travel times.

Figures 6 and 7 plot histograms of ISC *SS-S* and *ScS-S* differential times versus times obtained by Woodward and Masters (1991a,b) from long-period waveforms. Although the ISC data show more scatter, with suitable windowing, binning and averaging ISC differential times exhibit geographic patterns similar to those recently obtained from long-period GDSN data. This is illustrated in Figures 8-11 which plot differential travel time residuals versus bounce point positions for both the ISC and GDSN. Residuals have been smoothed by averaging within caps of 5° radius. Positive residuals are shown as triangles, negative residuals as crosses, with the size of the symbol proportional to the magnitude of the anomaly. Notice the coherent patterns of residuals in both data sets indicative of upper mantle heterogeneity in the case of *SS-S* and lowermost mantle heterogeneity and/or core-mantle-boundary topography in the case of *ScS-S*. This suggests that the ISC data can be used to map the shear velocity structure of the mantle, although the geographic coverage of the binned ISC data is less complete than that of the long-period data. For the binned and averaged data, plots of ISC versus long-period differential times show a correlation with approximately unit slope (Figure 12). The considerable scatter in these plots could be due to errors in the ISC picks not removed by the averaging scheme, or may reflect differences in long-period versus short-period travel times.

We also extracted 78,210 *PP-P* differential times and 119,810 *PcP-P* times from picks tabulated by the ISC from 1964 to 1987. This was done by identifying pairs of picks from a station for a particular event, where each pick is within 20 s of the predicted arrival time. As in the case of the S-waves, differential travel time residuals versus bounce point position show large-scale coherent patterns indicative of mantle heterogeneity. With suitable windowing, binning and averaging, ISC *PP-P* times exhibit geographic patterns similar to those recently obtained by Woodward and Masters (1991a) from long-period GDSN data. This suggests that the ISC data can be used to map the *P*-wave velocity structure of the upper mantle, although the geographic coverage of the binned ISC data is less complete than that of the long-period data. *PcP* can only very rarely be identified in long-period data so the ISC data provide the best available source of global *PcP - P* times.

Woodward, R.L., and G. Masters, 1991a, Global upper mantle structure from long-period differential travel times, *J. Geophys. Res.*, 96, 6351-6377.

Woodward, R.L., and G. Masters, 1991b, Lower-mantle structure from ScS-S differential travel times, *Nature*, 352, 231-233.

PART 3: OUTER CORE STRUCTURE

Our goal was to use *PKP* travel time data from the International Seismological Centre (ISC) to constrain possible aspherical structure in Earth's outer core and compare these results with current analyses of anomalous splitting of normal modes which suggest such structure.

We examined travel times for core phases collected by the International Seismological Centre (ISC) from 1964 to 1987 in an attempt to either resolve or place upper bounds on hypothetical outer-core velocity structures. We extracted 50,297 *PKP(BC)* travel times (145° to 156° range), 15,286 *PKP(DF)* times (110° to 135°) and 16,963 *PKP(AB)* times (150° to 165). We excluded *PKP(DF)* at longer ranges to avoid contamination by possible inner-core structure. All picks were examined (i.e. the ISC phase identifications are discarded), corrected for ellipticity, and the Toy station corrections applied. The ISC earthquake locations and origin times were used; the events were not relocated. Zero depth events were excluded as well as picks which follow a likely P-wave pick on the same seismogram (this should eliminate most depth phases).

We binned the data into summary rays using 15° cells in turning point position and ray azimuth. A fairly coarse increment was used since the data are sparse and we are mostly interested in any low-order structure. Estimates for the residual within each bin were obtained by finding the peak in a heavily smoothed histogram of the residuals. Standard errors for these estimates were estimated with a bootstrap technique which randomly resamples the data. This method introduces less bias than simply computing the mean within some fixed window (which will tend to reduce the size of the anomaly).

Results of this procedure are shown in Figures 13-15. Positive residuals are shown in black (slow anomalies) and negative residuals are shown in gray (fast anomalies). The position of the turning point bin is indicated on the map, with the angle of the wedges showing the local ray azimuth at the turning points and the length of the wedge showing the size of the residual. Bins are only shown if the estimated standard error is less than 0.5 s. These plots reveal how sparse the ray coverage is (most of the turning point bins contain data from only one azimuth). However, there is coherence between adjacent summary rays suggesting that these times are indicative of structure in the mantle or core.

Recent analyses of anomalous splitting of normal mode spectral peaks (e.g., Ritzwoller *et al.*, 1986; Widmer *et al.*, 1992) have suggested the possibility of aspherical structure in Earth's outer core. The hypothesized models contain axi-symmetric velocity perturbations of spherical harmonic degree 2 in which velocities are about 0.5% faster near the poles than at the equator (i.e. a C_{20} anomaly). These models predict travel time anomalies of several seconds in *PKP* phases which travel through the outer core. However, the *PKP* times plotted in Figures 13-15 do not exhibit obvious C_{20} anomalies. Plots of predicted vs. actual PKP travel times show large scatter with no clear correlation. Figure 16 shows the change in misfit variance when the data are corrected for an outer core velocity model which can explain the anomalous splitting data. The solid line is for *PKP(DF)*, the long-dashed line for *PKP(BC)* and the short dashed line for *PKP(AB)*. The outer core model increases the data variance by 50 to 80%.

These results did not use any correction for mantle heterogeneity. We experimented with scaled versions of shear-wave models but found that these did not predict ISC *P*-wave

residuals very well. Instead, we used LO2.56, the Harvard lower mantle *P*-wave model. Figure 17 shows the variance change which results when this model is applied to *P* and *PKP* data. The *P* analysis used 35,300 picks from 85 to 100°, binned and averaged exactly the same way as the *PKP* data. LO2.56 reduced the variance of these data by about 20%. The best variance reduction for *P* was achieved with a scaling of unity, indicating that the model amplitude is about right. The results for *P* are reassuring since LO2.56 is based on ISC *P*-wave data; however it is somewhat disturbing that a greater variance reduction is not achieved. Figure 17 also shows the results of applying this model to *PKP* data – the variance of these data are increased by 40 to 50%. A tiny variance reduction can be achieved if LO2.56 is reduced in size by about a factor of 5.

As an experiment, we went ahead and applied a correction to the *PKP* times based on the full LO2.56 model. However in light of the large variance increase that results, it is questionable whether this should be done. Figure 18 is analogous to Figure 16 and shows the variance change as a function of C_{20} anomaly size for the LO2.56 corrected data. The mantle corrections do not have a large affect on the results.

Our analysis of PKP travel times from the ISC found that they appear inconsistent with outer core velocity anomalies of the size required to explain anomalous mode splitting data. We are currently exploring the effect of confining the anomaly to particular depth ranges within the outer core. Preliminary results indicate that the ISC data are less inconsistent with models in which the anomaly is confined to near the surface of the outer core, but that this improvement is nevertheless too small to reconcile the travel time and mode data. We are also experimenting with outer core anisotropy models and higher order heterogeneity models. However, so far the source of the bulk of the anomalous mode splitting remains unknown.

The need to correct core phase data for the effects of mantle heterogeneity is a problem in these analyses. Most of the coherent signal in *PKP* data is probably due to mantle heterogeneity; however current mantle models do not account for the signal. This is most likely due to limitations in the mantle models rather than an indication of core structure. A promising approach for future analyses will be to include both *P* and *PKP* data in inversions for mantle velocity structure to see if a model can be found which is consistent with both data sets.

Ritzwoller, M., G. Masters, and F. Gilbert, 1986, Observations of anomalous splitting and their interpretation in terms of aspherical structure, *J. Geophys. Res.*, **91**, 10203-10228.

Widmer, R., G. Masters, and F. Gilbert, 1992, Observably split multiplets—data analysis and interpretation in terms of large-scale aspherical structure, *Geophys. J. Int.*, **111**, 559-576.

PART 4: SOFTWARE DEVELOPMENT

We have developed computer programs to return travel time and ray geometries for a given seismic phase and source-receiver pair. For speed and convenience we have implemented a set of subroutines for the radially symmetric earth which interpolate travel

times from a set of tables. We have computed these tables for dozens of seismic phases using both PREM and the new IASPEI91 earth models. In addition, we have digitized the JB tables for most of the major phases. We have written a subroutine, GET_TT, which automatically returns a travel time for a given phase name, range, and source depth. We have incorporated this subroutine in our data analysis software here at IGPP.

We have written a subroutine, GET_PATH, which returns a ray path (specified by depth, range and accumulated travel time at 10 km depth increments) for a given phase name, range and source depth. We have also implemented a subroutine, GET_PERT, which returns the accumulated travel time anomaly for ray paths determined from GET_PATH and global 3-d earth models specified by their spherical harmonic expansions. We have implemented these routines for several mantle models (e.g. LO2.56, M84c, sh.10c.17, MDSLH) after putting them into a standard format. These subroutines will be incorporated into our data analysis software here at IGPP, such that as a seismogram is displayed on the screen the predicted travel times for all major seismic phases for any 3-d earth model will also be shown for comparison purposes.

Figures

Figure 1. *PKP(BC) – PKP(DF)* differential travel time residuals from ISC data plotted as a function of range. No points are found in the lower left corner due to the impossibility of observing negative *BC – DF* times (the first arrival is always assumed to be *DF*). Notice that ISC picks are to the nearest 0.1 s and that operators tend to pick even seconds and half seconds; this causes the pronounced diagonal banding in the data.

Figure 2. ISC differential *PKP(BC) - PKP(DF)* travel time residuals plotted on a map of turning point position. Data have been binned and averaged into approximately equal area bins, with a minimum of three rays required in each averaging bin.

Figure 3. ISC differential *PKP(BC) - PKP(DF)* travel time residuals plotted on a map of ray direction at the turning point. Note the generally positive residuals near the north and south poles. The slight deviations from 180° symmetry result from asymmetries in the binning scheme.

Figure 4. ISC travel times from 1964 to 1987 for shallow events (<50 km).

Figure 5. ISC travel times relative to an *S*-wave pick within 20 s of the theoretical *S* arrival time. Only shallow events are plotted (<50 km).

Figure 6. Histograms of *SS-S* residuals obtained from long-period GDSN waveforms (left) and ISC picks (right).

Figure 7. Histograms of *ScS-S* residuals obtained from long-period GDSN waveforms (left) and ISC picks (right).

Figure 8. ISC *SS-S* residuals binned and averaged in 5° radius caps by turning point position. Negative (fast) anomalies are shown as triangles; positive (slow) anomalies are shown as plus signs.

Figure 9. GDSN *SS-S* residuals binned and averaged in 5° radius caps by turning point position. Negative (fast) anomalies are shown as triangles; positive (slow) anomalies are shown as plus signs.

Figure 10. ISC *ScS-S* residuals binned and averaged in 5° radius caps by turning point position. Negative (fast) anomalies are shown as triangles; positive (slow) anomalies are shown as plus signs.

Figure 11. GDSN *ScS-S* residuals binned and averaged in 5° radius caps by turning point position. Negative (fast) anomalies are shown as triangles; positive (slow) anomalies are shown as plus signs.

Figure 12. ISC versus GDSN differential time residuals for *SS-S* and *ScS-S* (right).

Figure 13. *PKP(BC)* residuals binned and plotted at turning point location. Positive (slow) anomalies are shown as black, negative (fast) anomalies as gray. Azimuth of ray at turning point is indicated by the angle of the plot. Only residuals with estimated standard errors less than 0.5 s are plotted.

Figure 14. *PKP(DF)* residuals binned and plotted at turning point location. Positive (slow) anomalies are shown as black, negative (fast) anomalies as gray. Azimuth of ray at turning point is indicated by the angle of the plot. Only residuals with estimated standard errors less than 0.5 s are plotted.

Figure 15. *PKP(AB)* residuals binned and plotted at turning point location. Positive (slow) anomalies are shown as black, negative (fast) anomalies as gray. Azimuth of ray at turning point is indicated by the angle of the plot. Only residuals with estimated standard errors less than 0.5 s are plotted.

Figure 16. Variance of misfit to ISC residual bins as a function of relative size of outer core C_{20} velocity heterogeneity. *PKP(DF)* is shown as a solid line, *PKP(BC)* as a dashed line, and *PKP(AB)* as a dotted line. A C_{20} anomaly which can explain the mode splitting data (scaled to a relative size of unity) increases the variance of the ISC data by 50 to 80%.

Figure 17. Variance of misfit to ISC residual bins as a function of the relative size of the mantle heterogeneity model LO2.56. This model improves the fit to the *P*-wave data but increases the scatter in *PKP* travel times.

Figure 18. Variance of misfit to LO2.56 corrected ISC residual bins as a function of relative size of outer core C_{20} velocity heterogeneity. *PKP(DF)* is shown as a solid line, *PKP(BC)* as a dashed line, and *PKP(AB)* as a dotted line. The mantle corrections do not greatly change the results (compare Figures 16 and 18).

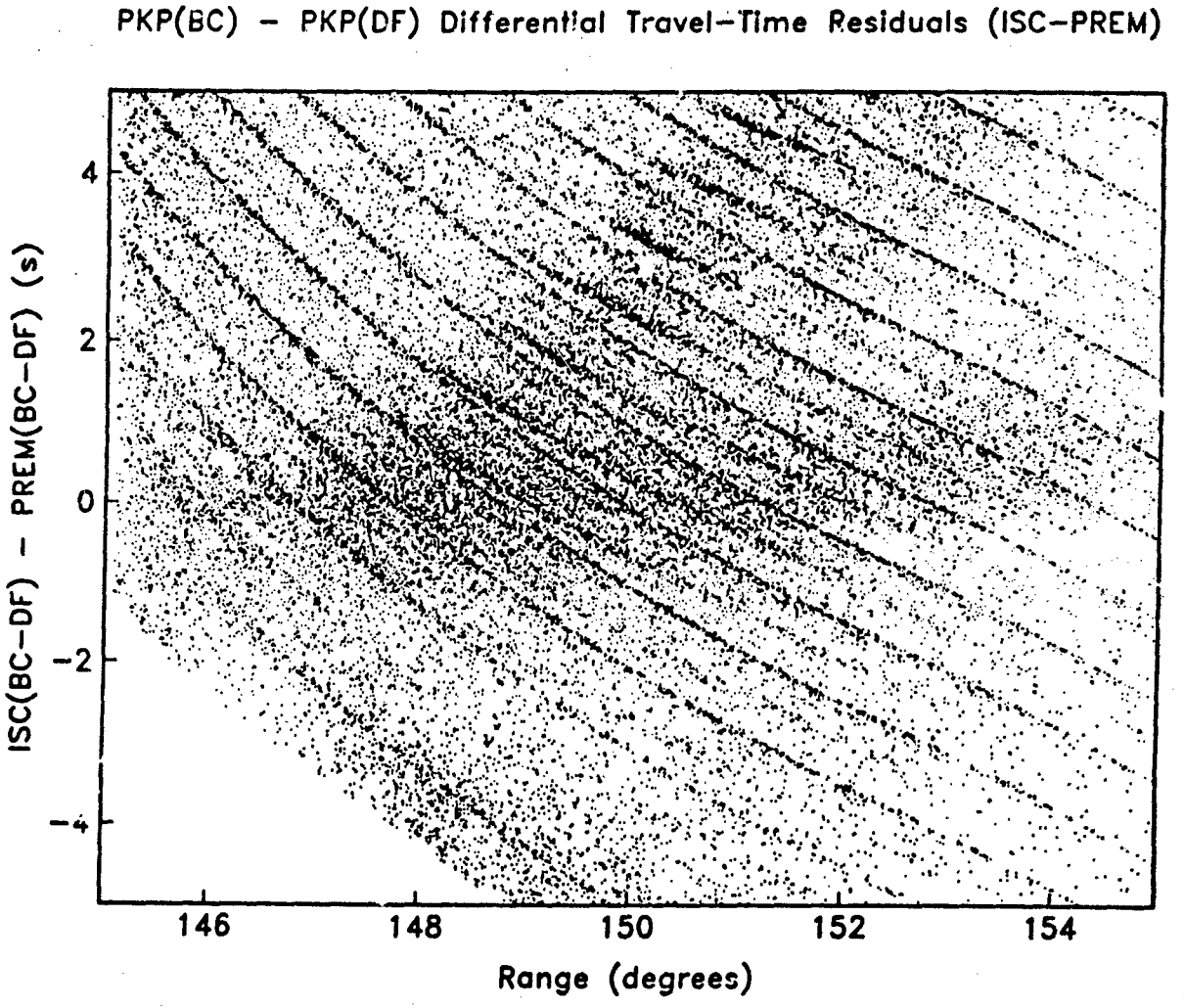
PKP(BC) – PKP(DF) Differential Travel–Time Residuals (ISC–PREM)
ISC(BC–DF) – PREM(BC–DF) (s)
4
2
0
–2
–4
146
148
150
152
154
Range (degrees)

Figure 1.

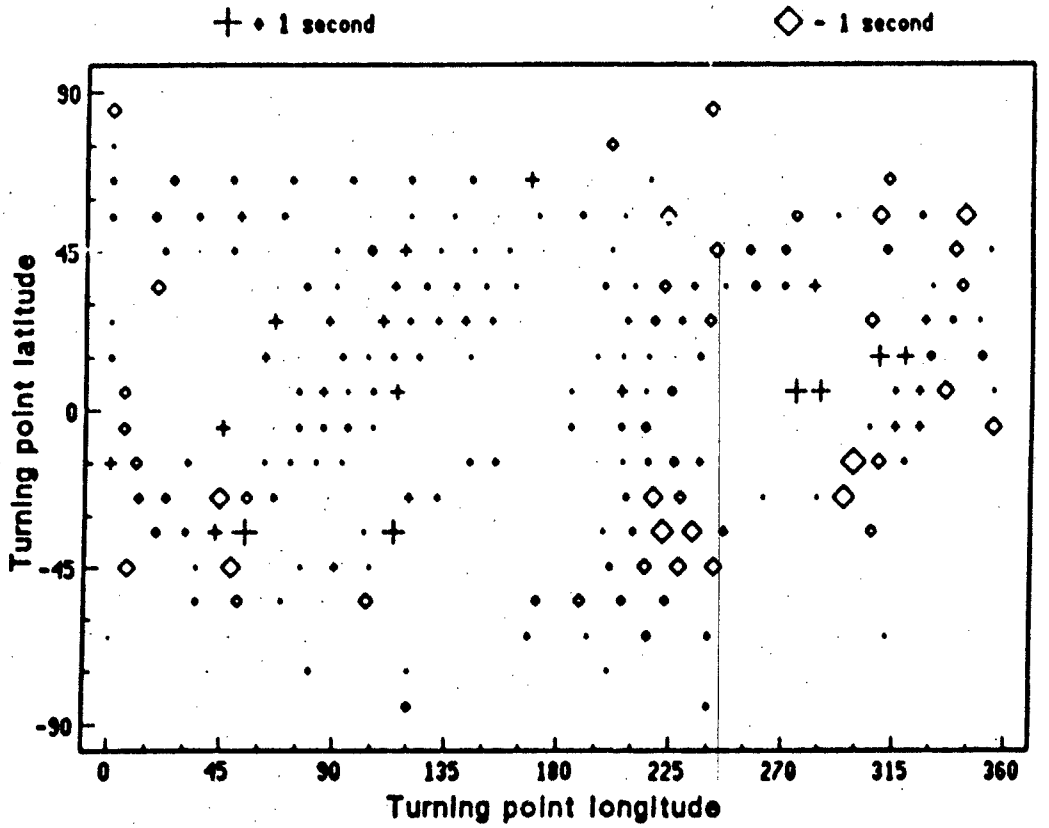
+ = 1 second
◇ = -1 second
90
45
0
-45
-90
Turning point latitude
0
45
90
135
180
225
270
315
360
Turning point longitude

Figure 2.

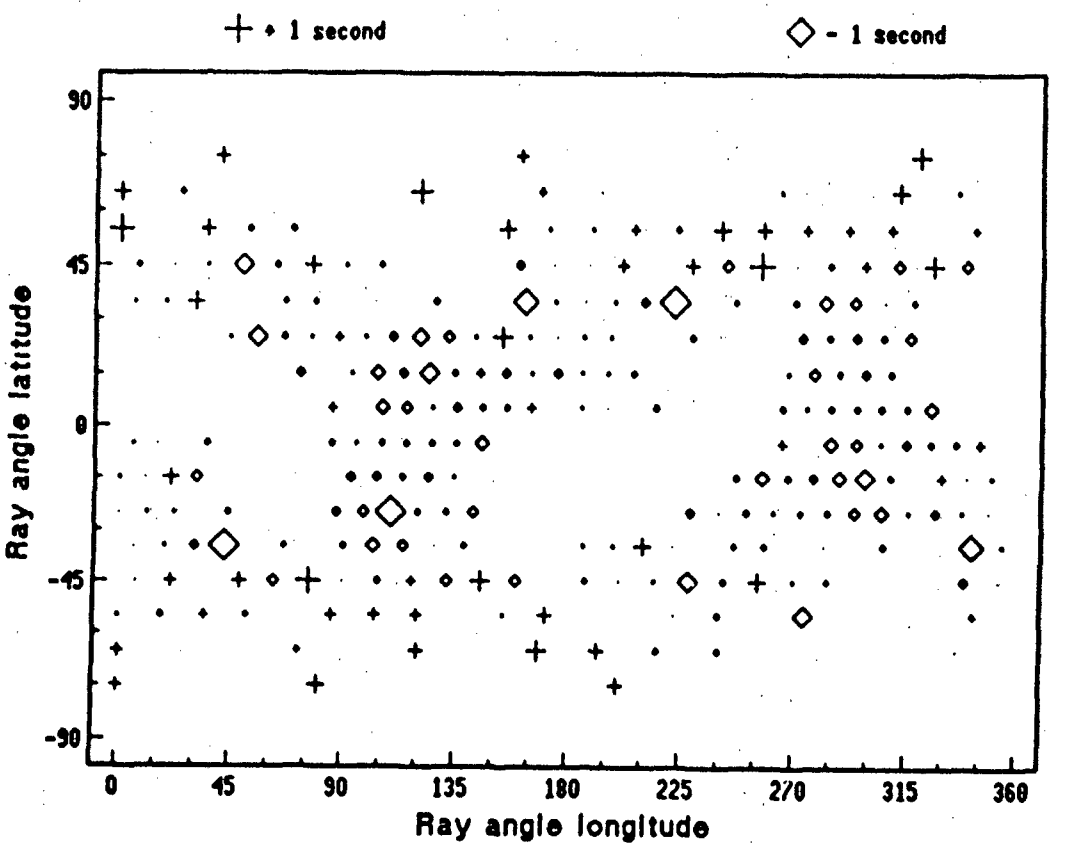
+ = 1 second
◇ = -1 second
90
45
0
-45
-90
Ray angle latitude
0
45
90
135
180
225
270
315
360
Ray angle longitude

Figure 3.

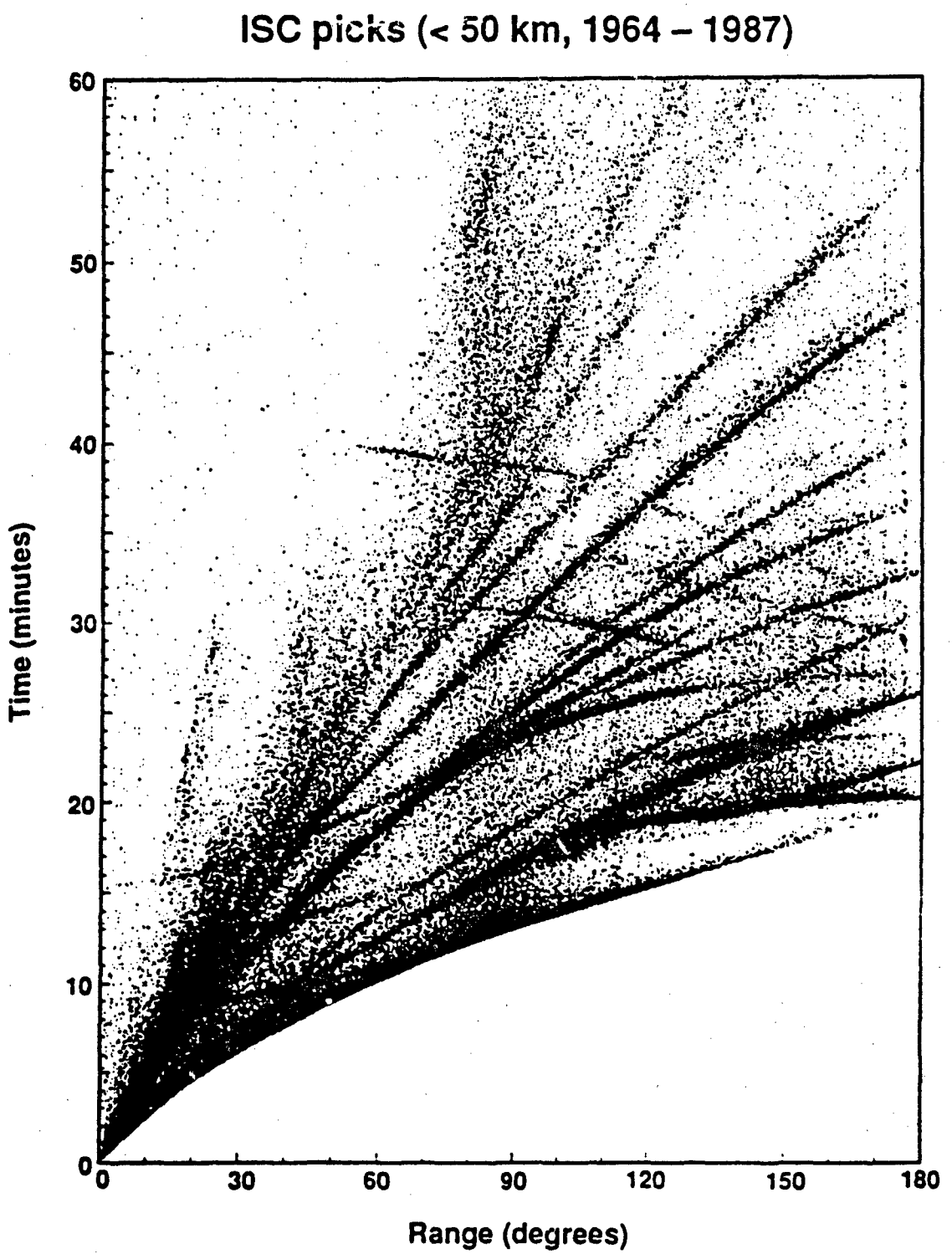
ISC picks (< 50 km, 1964 – 1987)
Time (minutes)
0
10
20
30
40
50
60
0
30
60
90
120
150
180
Range (degrees)

Figure 4.

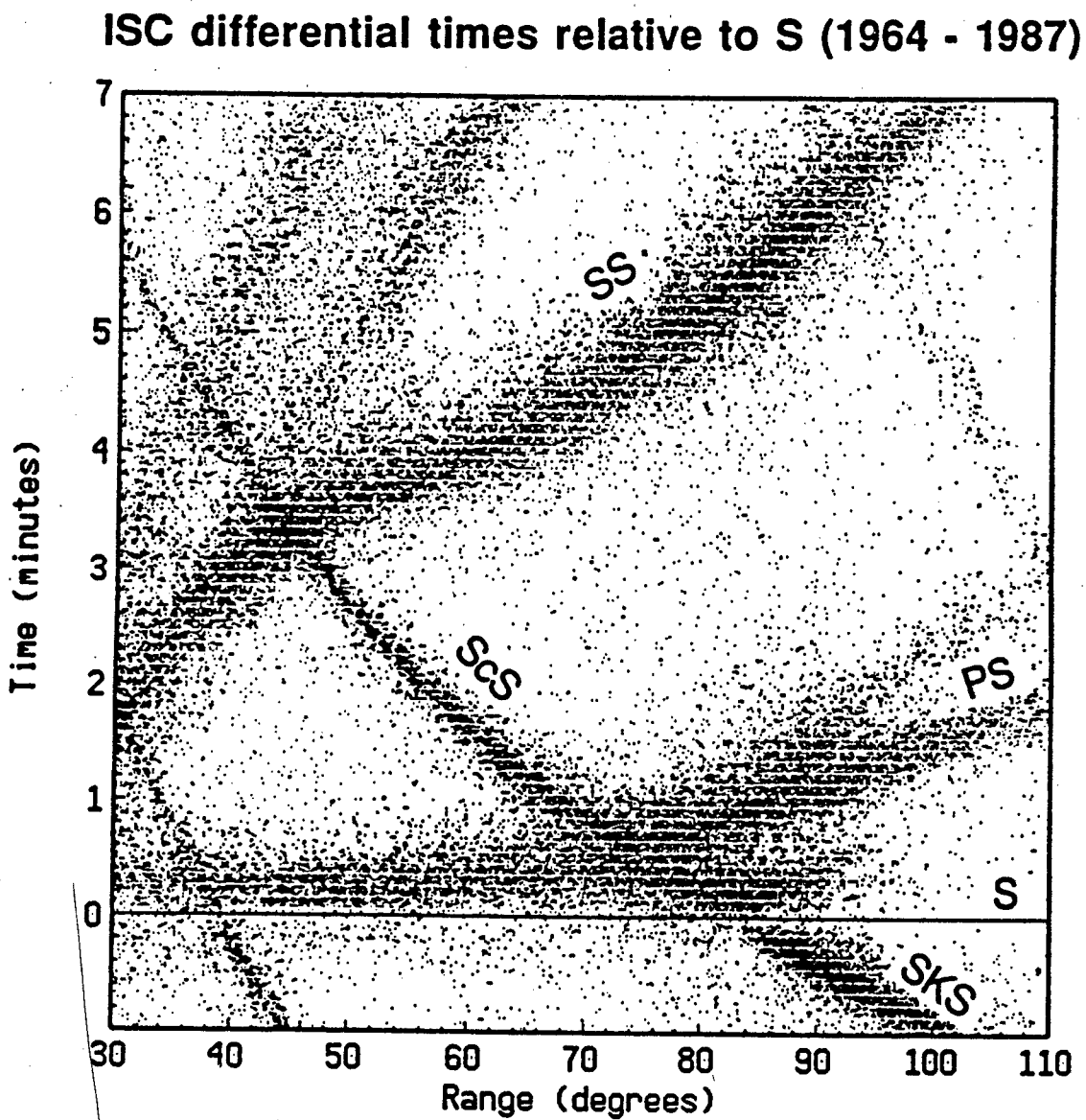
ISC differential times relative to S (1964 - 1987)
Time (minutes)
7
6
5
4
3
2
1
0
SS
SCS
PS
S
SKS
30
40
50
60
70
80
90
100
110
Range (degrees)

Figure 5.

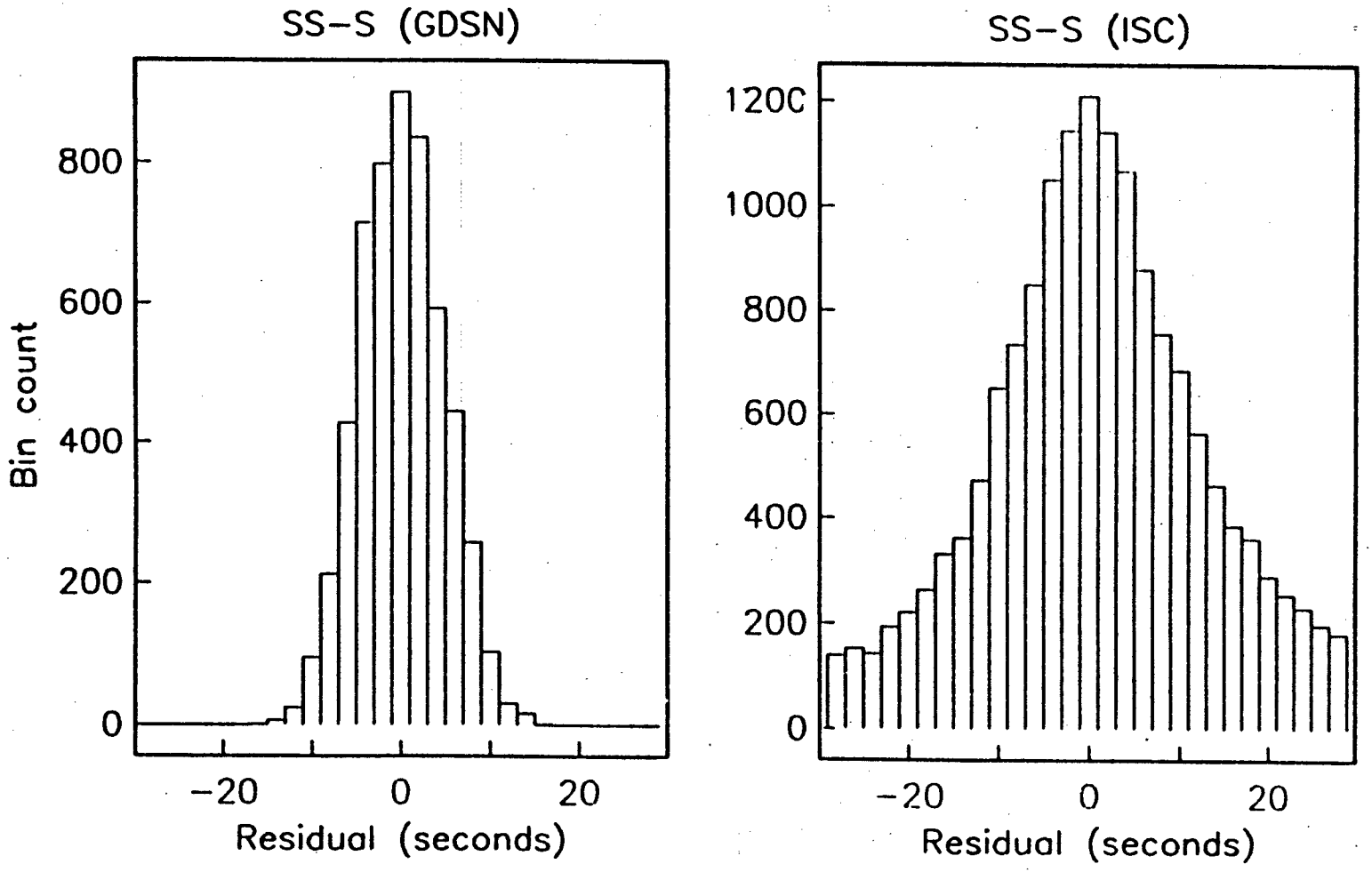
SS–S (GDSN)
SS–S (ISC)
Bin count
800
600
400
200
0
1200
1000
800
600
400
200
0
–20
0
20
Residual (seconds)
–20
0
20
Residual (seconds)

Figure 6.

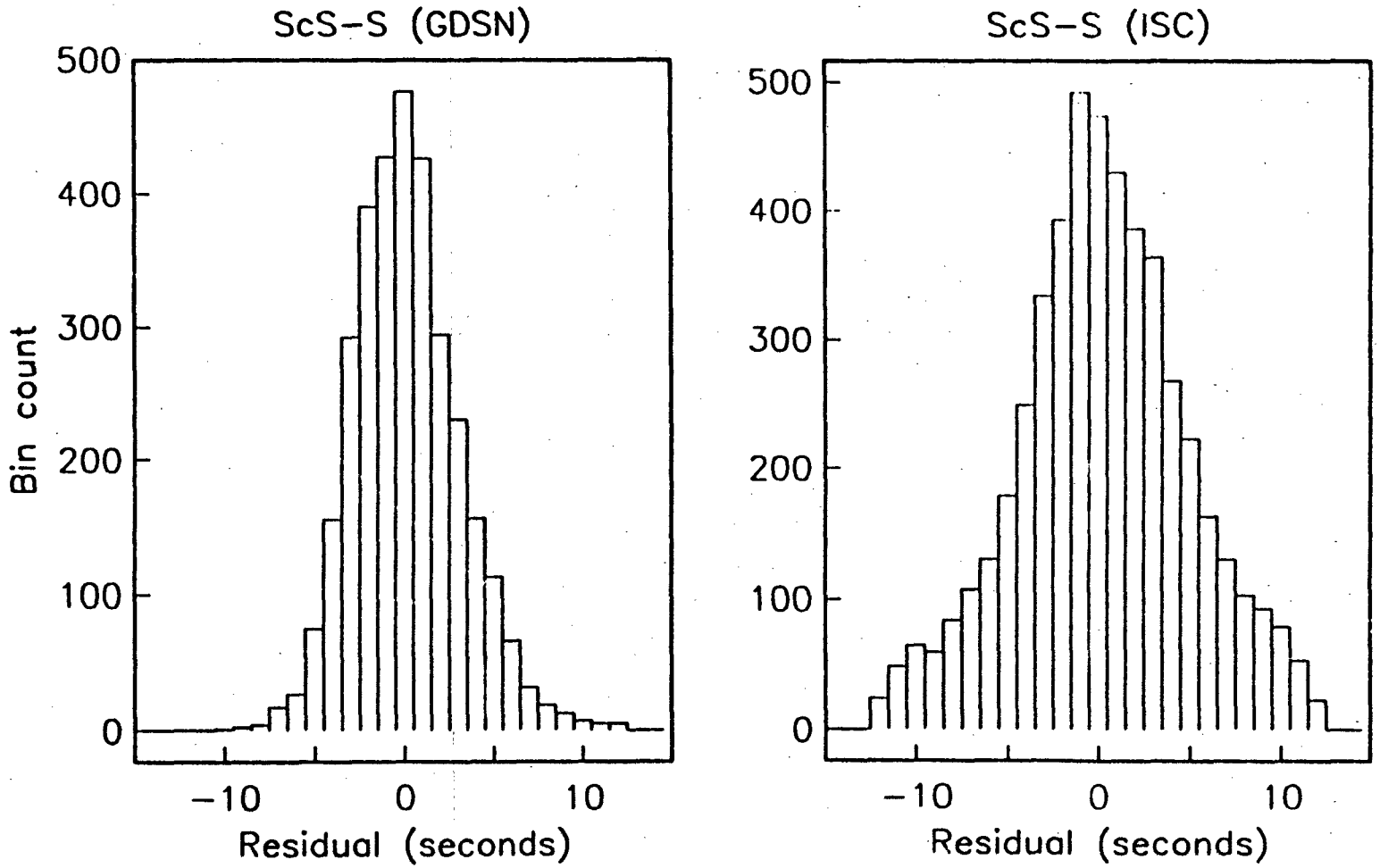
ScS–S (GDSN)
ScS–S (ISC)
Bin count
500
400
300
200
100
0
–10
0
10
Residual (seconds)

Figure 7.

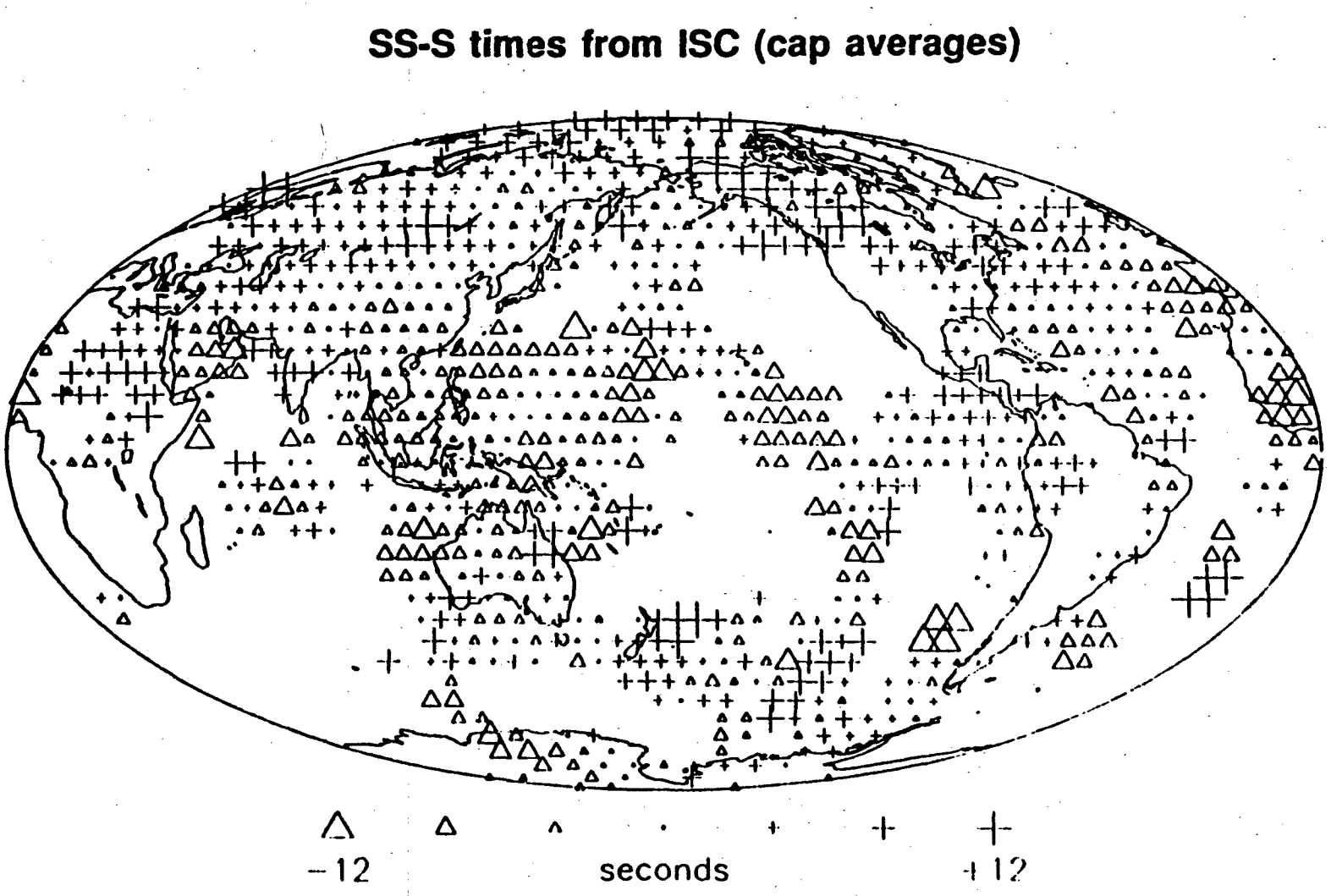

Figure 8.

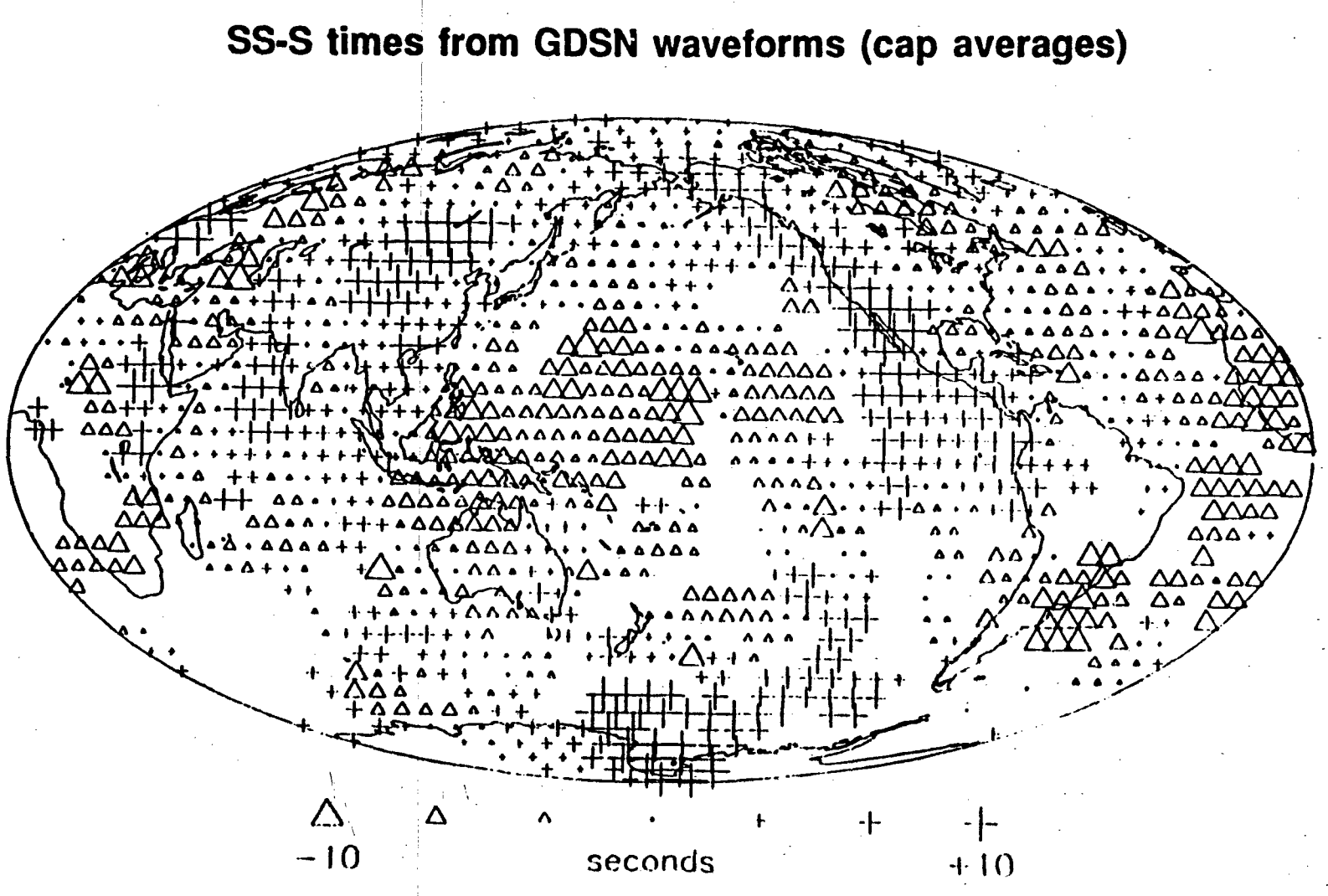

Figure 9.

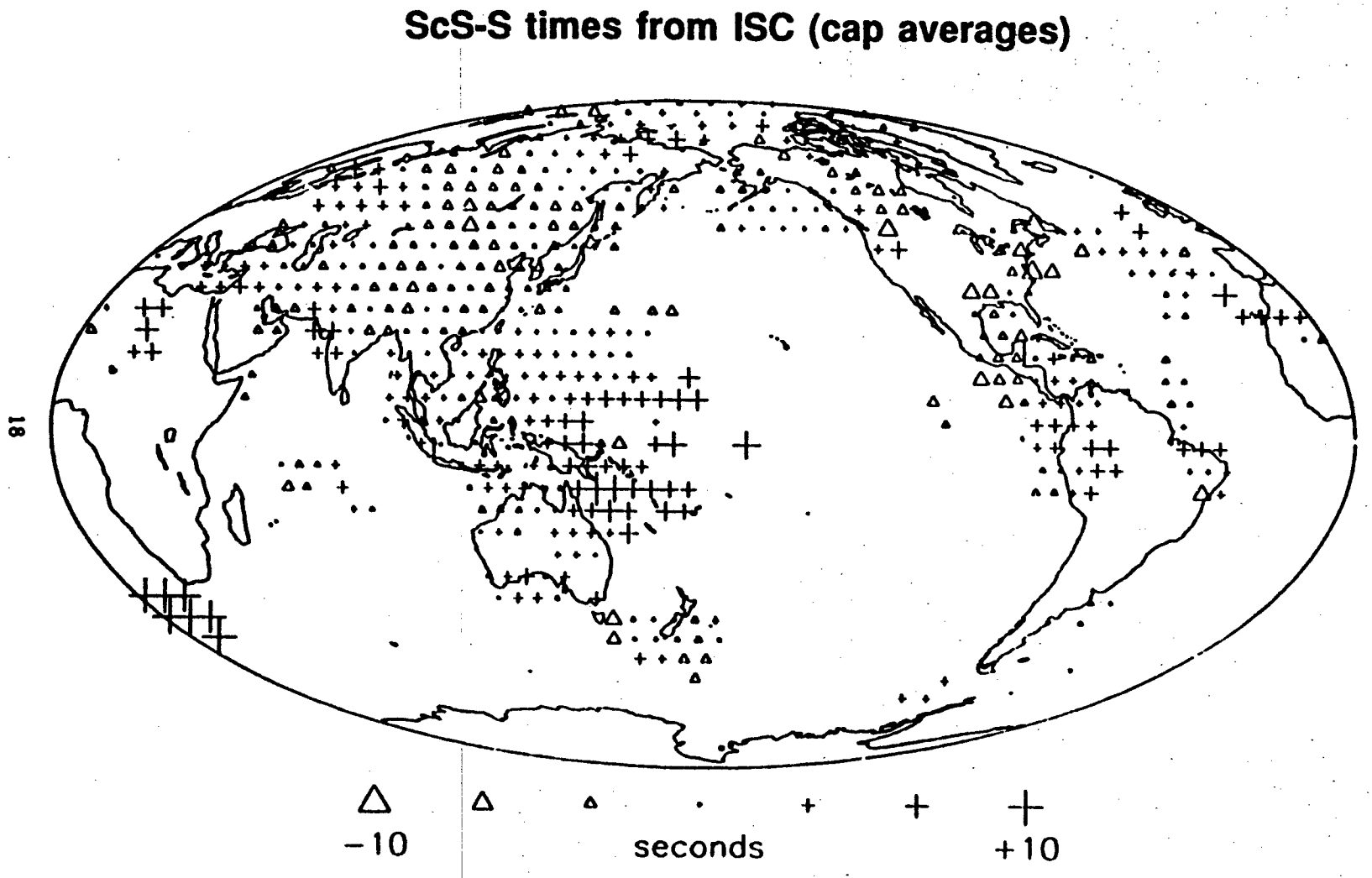

Figure 10.

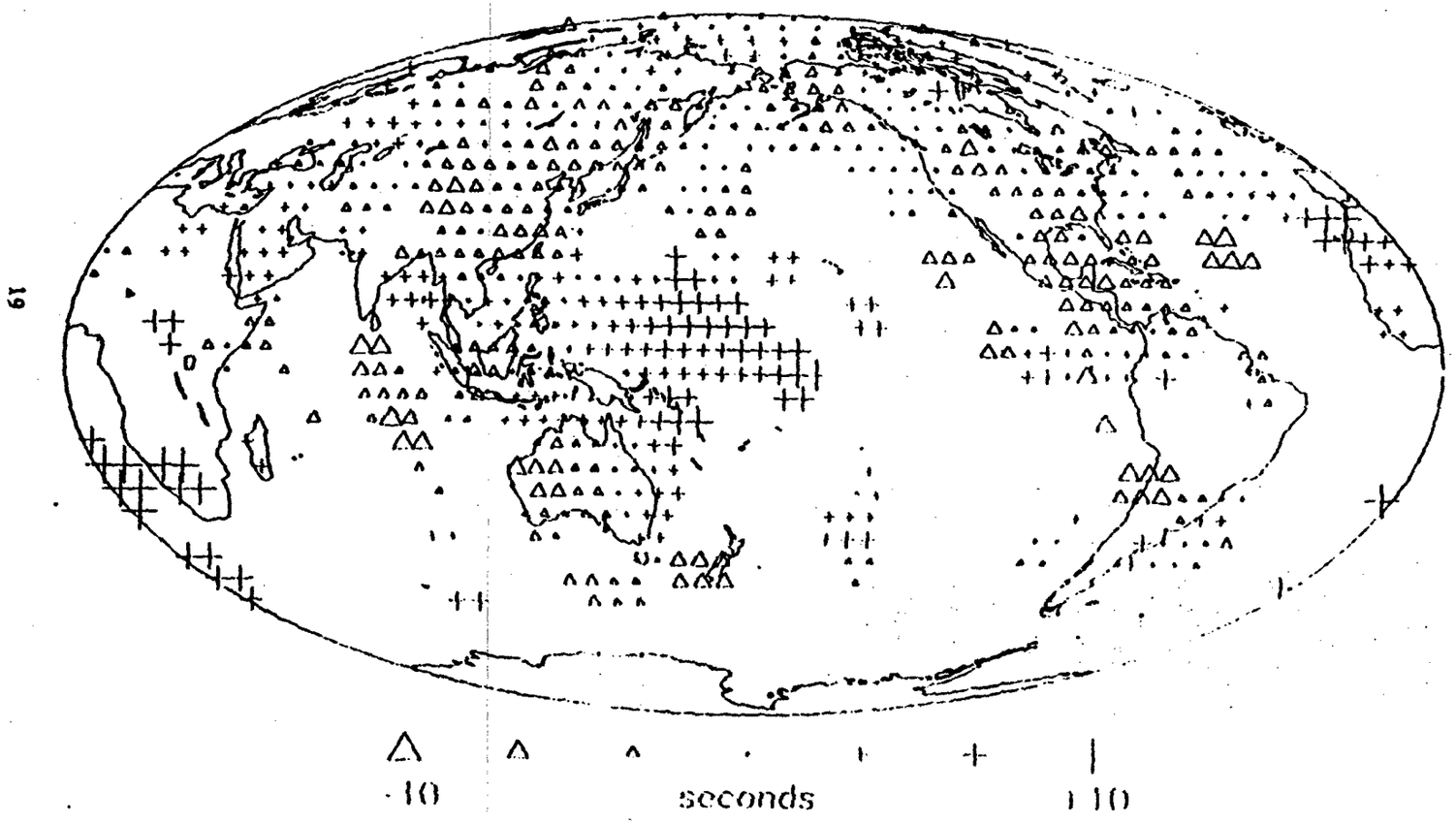
ScS-S times from GDSN waveforms (cap averages)
19
0
-10
seconds
10

Figure 11.

GDSN versus ISC differential times (cap averages)

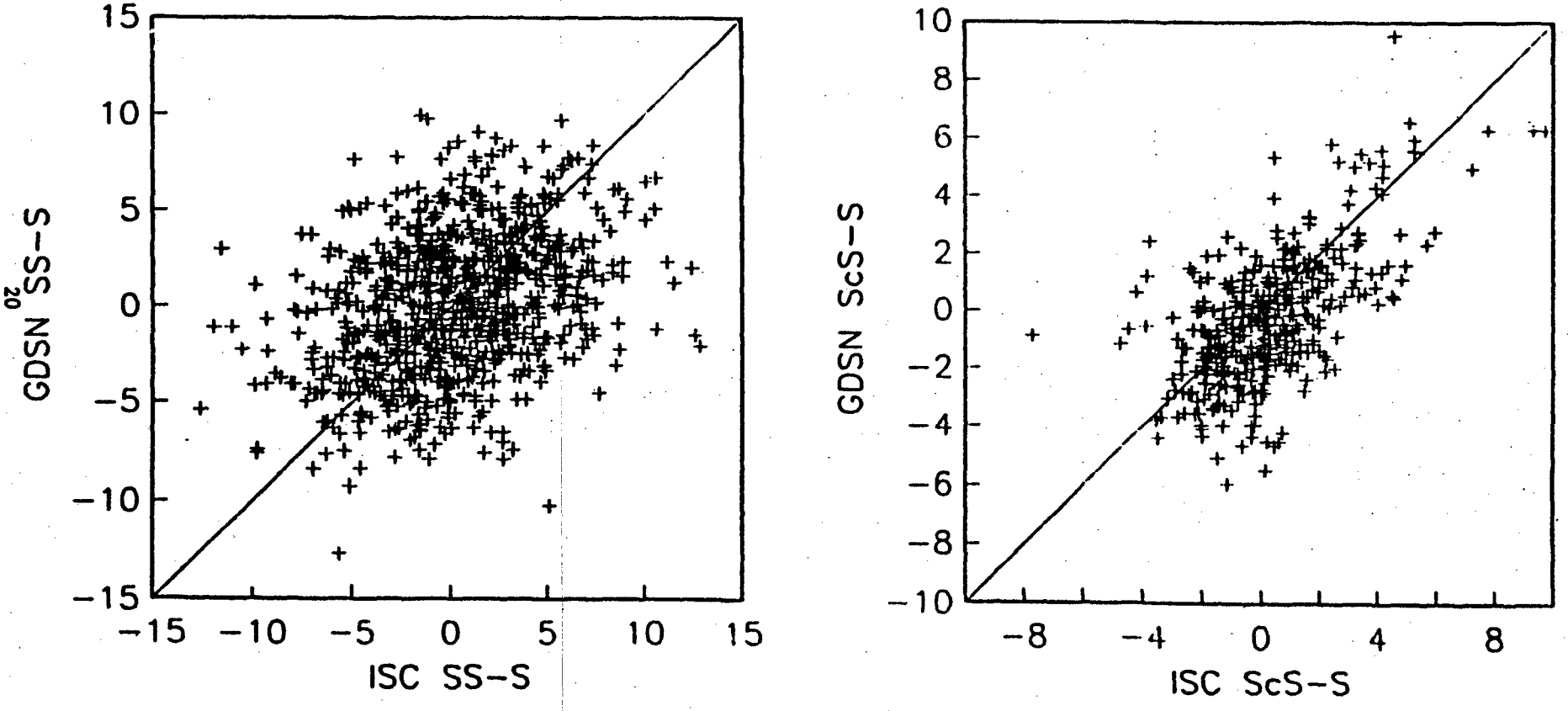

Figure 12.

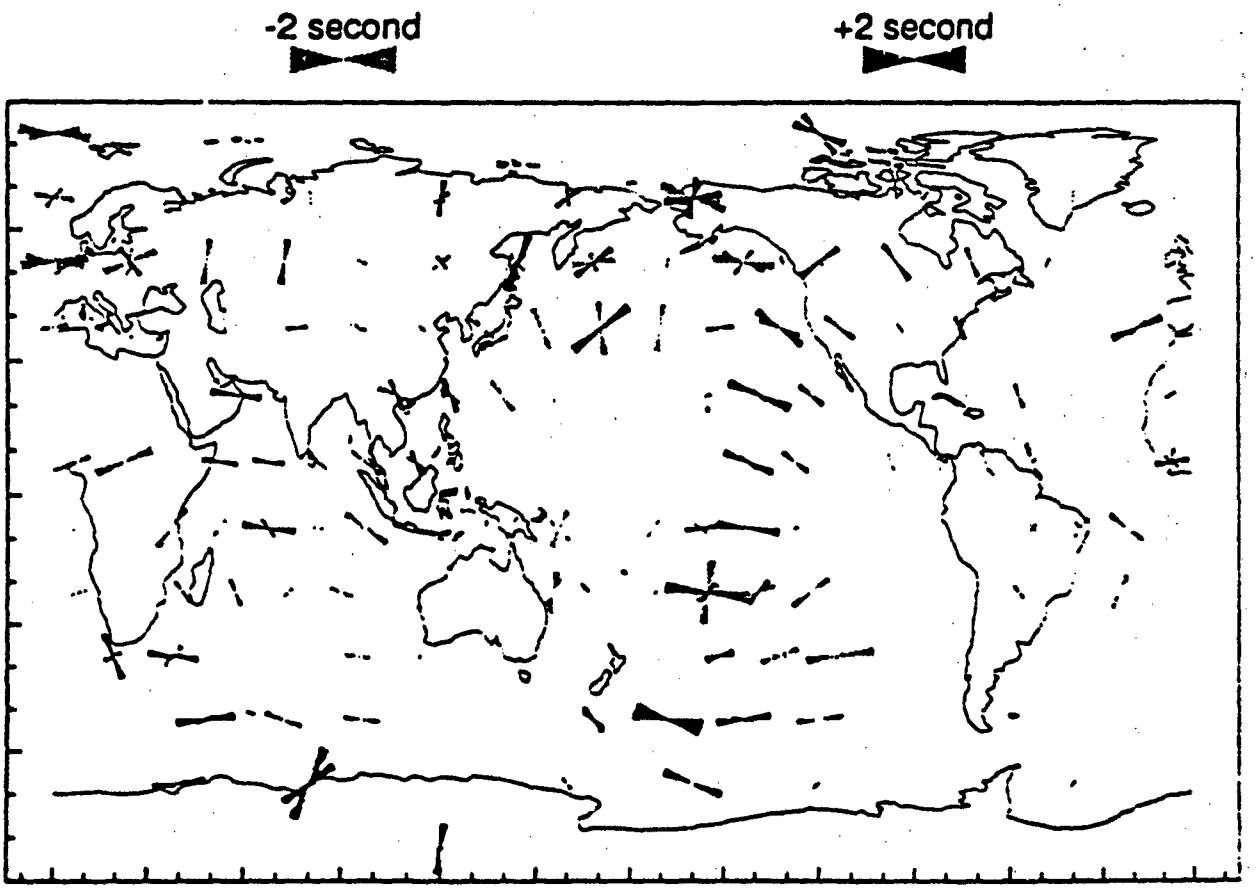

Figure 13.

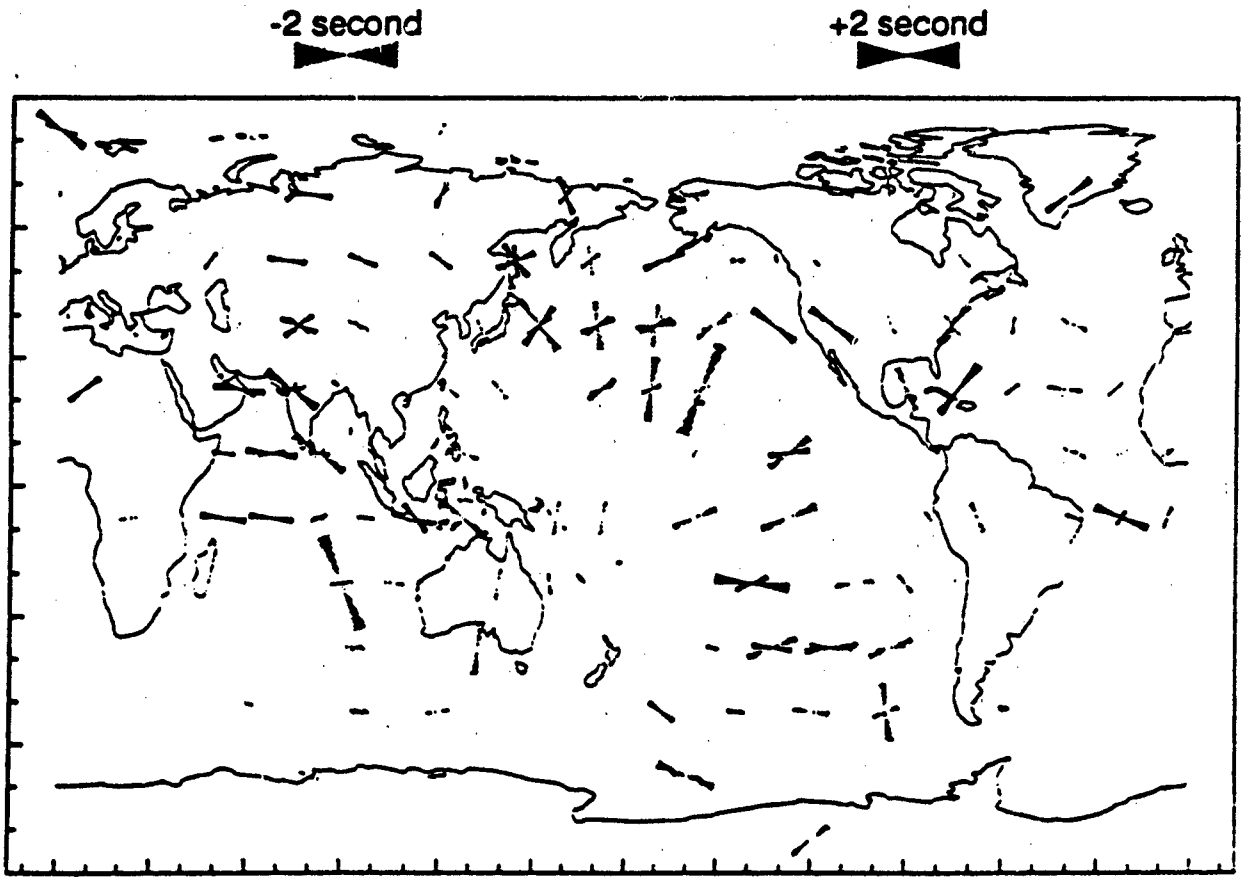

Figure 14.

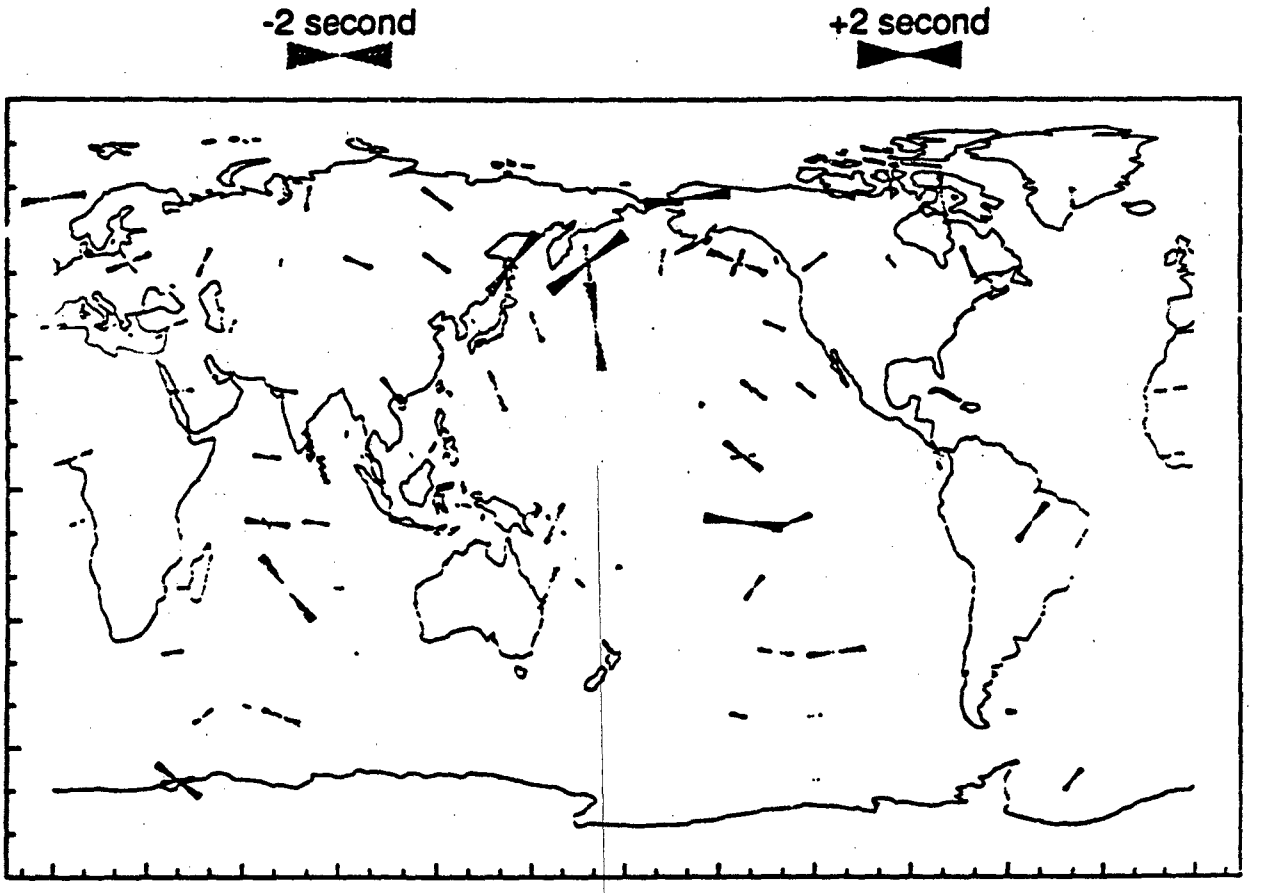

Figure 15.

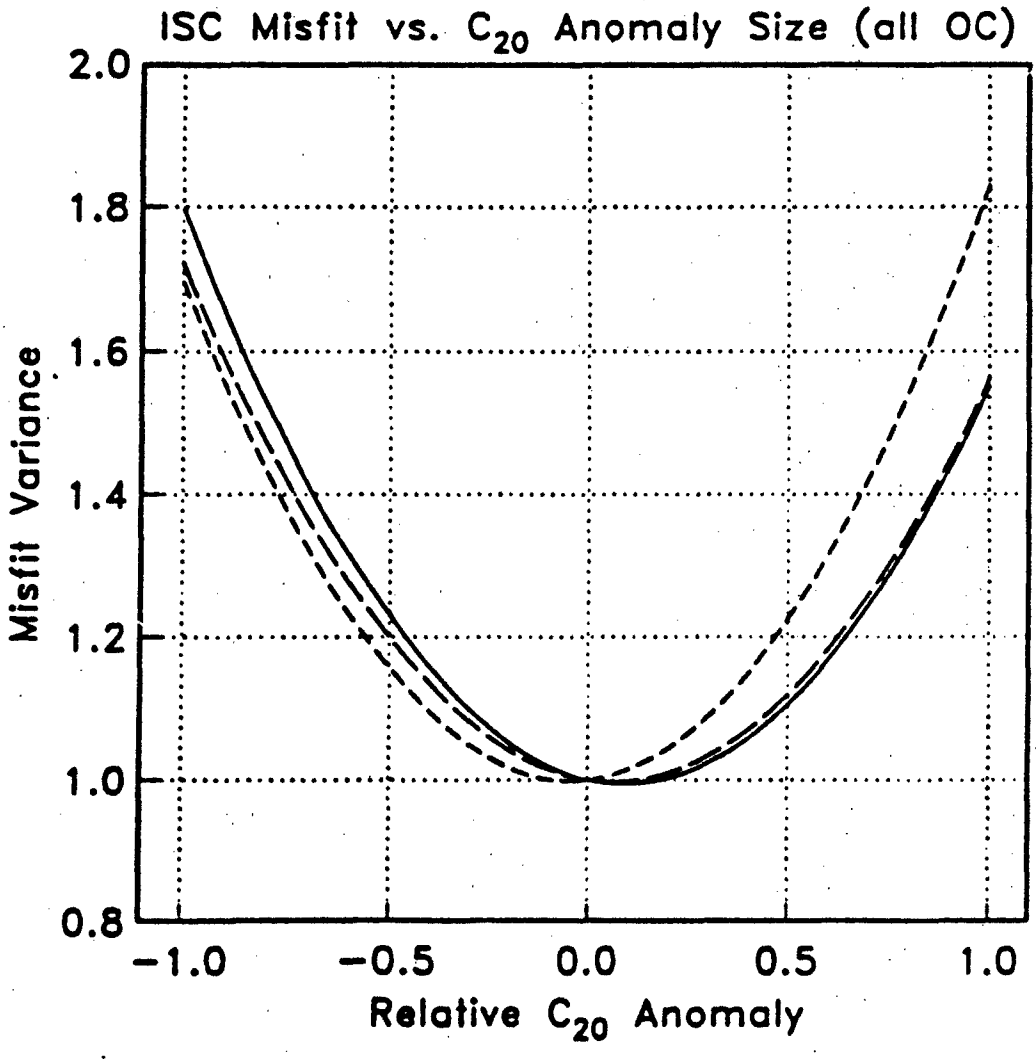
ISC Misfit vs. C_{20} Anomaly Size (all OC)
2.0
1.8
1.6
1.4
1.2
1.0
0.8
Misfit Variance
−1.0
−0.5
0.0
0.5
1.0
Relative C_{20} Anomaly

Figure 16.

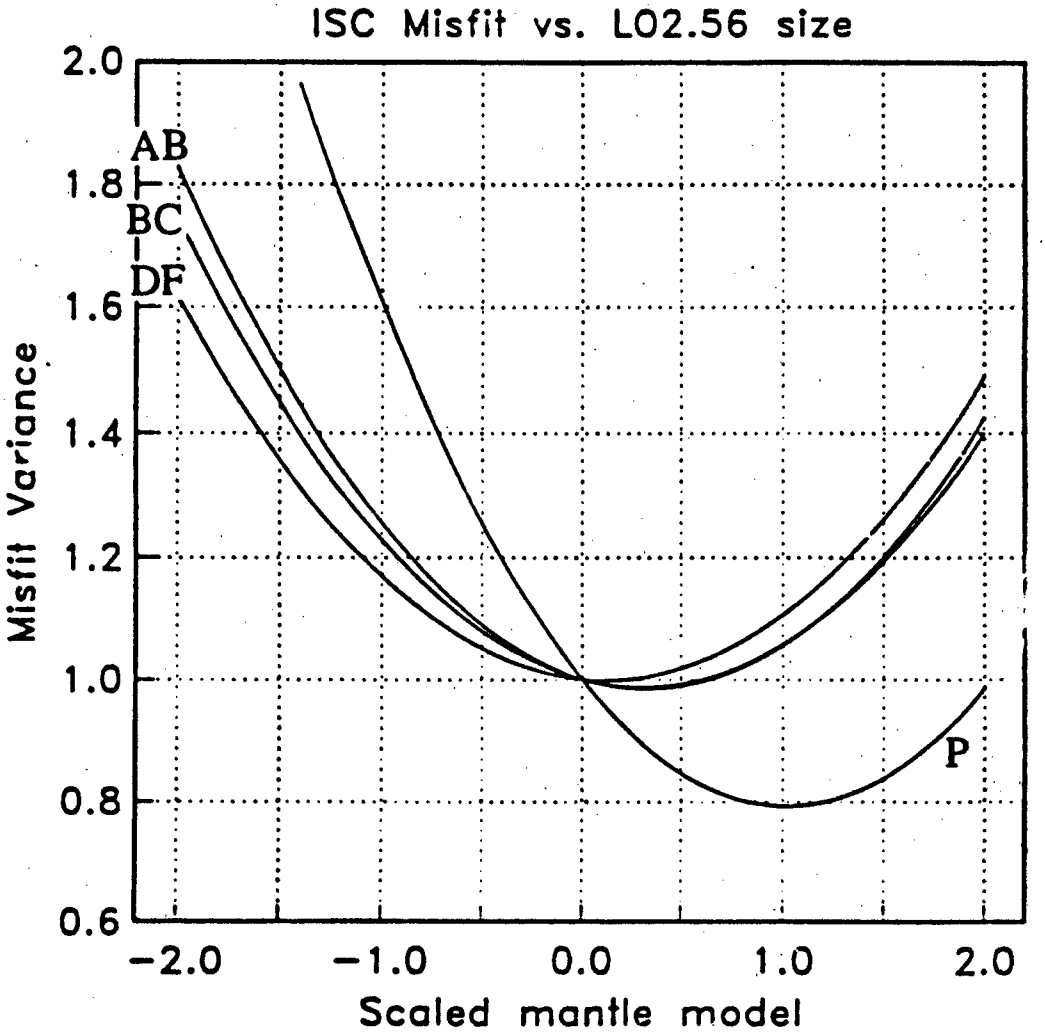
ISC Misfit vs. LO2.56 size
2.0
1.8
1.6
1.4
1.2
1.0
0.8
0.6
Misfit Variance
AB
BC
DF
P
−2.0
−1.0
0.0
1.0
2.0
Scaled mantle model

Figure 17.

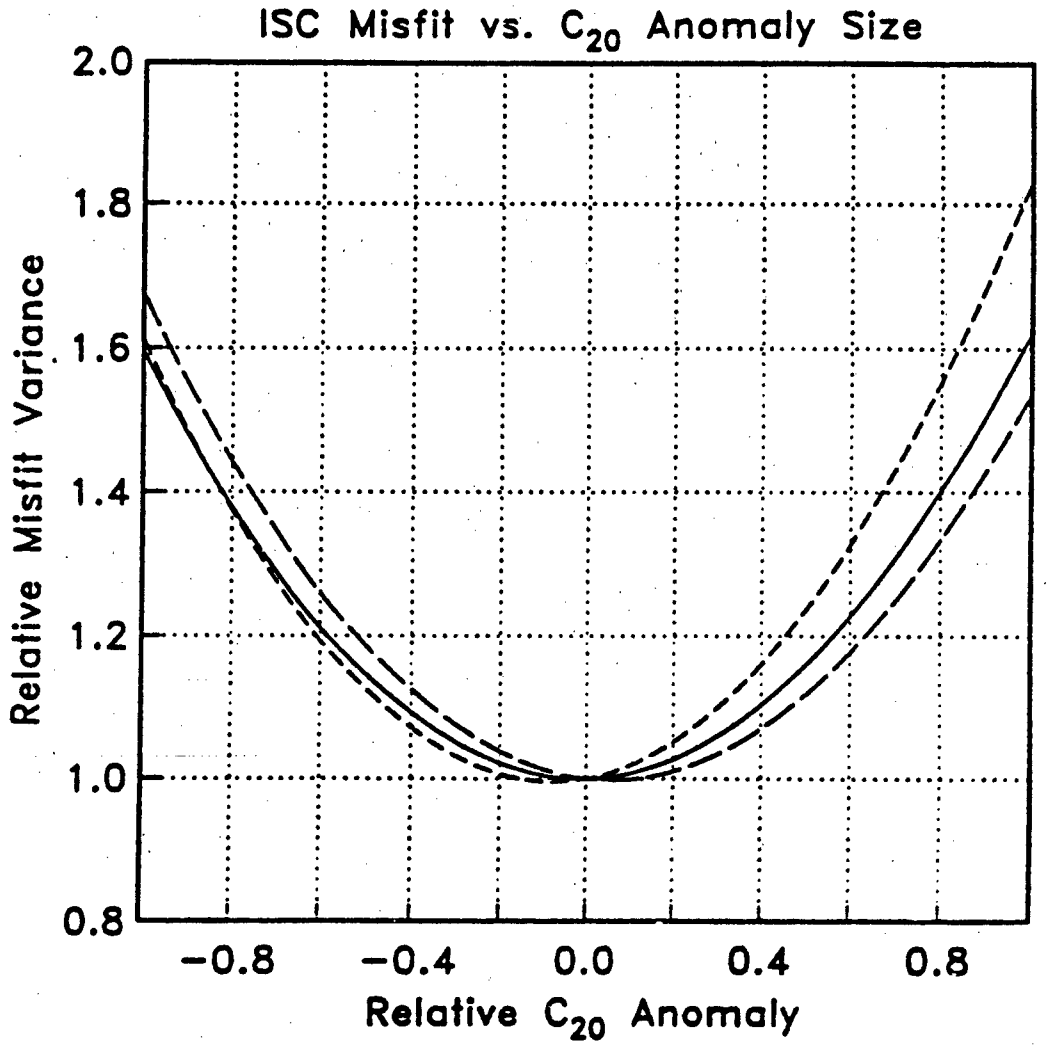
ISC Misfit vs. C_{20} Anomaly Size
Relative Misfit Variance
2.0
1.8
1.6
1.4
1.2
1.0
0.8
−0.8
−0.4
0.0
0.4
0.8
Relative C_{20} Anomaly

Figure 18

Prof. Thomas Ahrens
Seismological Lab, 252-21
Division of Geological & Planetary Sciences
California Institute of Technology
Pasadena, CA 91125

Prof. Keiiti Aki
Center for Earth Sciences
University of Southern California
University Park
Los Angeles, CA 90089-0741

Prof. Shelton Alexander
Geosciences Department
403 Deike Building
The Pennsylvania State University
University Park, PA 16802

Dr. Ralph Alewine, III
DARPA/NMRO
3701 North Fairfax Drive
Arlington, VA 22203-1714

Prof. Charles B. Archambeau
CIRES
University of Colorado
Boulder, CO 80309

Dr. Thomas C. Bache, Jr.
Science Applications Int'l Corp.
10260 Campus Point Drive
San Diego, CA 92121 (2 copies)

Prof. Muawia Barazangi
Institute for the Study of the Continent
Cornell University
Ithaca, NY 14853

Dr. Jeff Barker
Department of Geological Sciences
State University of New York
at Binghamton
Vestal, NY 13901

Dr. Douglas R. Baumgardt
ENSCO, Inc
5400 Port Royal Road
Springfield, VA 22151-2388

Dr. Susan Beck
Department of Geosciences
Building #77
University of Arizona
Tuscon, AZ 85721

Dr. T.J. Bennett
S-CUBED
A Division of Maxwell Laboratories
11800 Sunrise Valley Drive, Suite 1212
Reston, VA 22091

Dr. Robert Blandford
AFTAC/TT, Center for Seismic Studies
1300 North 17th Street
Suite 1450
Arlington, VA 22209-2308

Dr. Stephen Bratt
Center for Seismic Studies
1300 North 17th Street
Suite 1450
Arlington, VA 22209-2308

Dr. Lawrence Burdick
Woodward-Clyde Consultants
566 El Dorado Street
Pasadena, CA 91109-3245

Dr. Robert Burridge
Schlumberger-Doll Research Center
Old Quarry Road
Ridgefield, CT 06877

Dr. Jerry Carter
Center for Seismic Studies
1300 North 17th Street
Suite 1450
Arlington, VA 22209-2308

Dr. Eric Chael
Division 9241
Sandia Laboratory
Albuquerque, NM 87185

Dr. Martin Chapman
Department of Geological Sciences
Virginia Polytechnical Institute
21044 Derring Hall
Blacksburg, VA 24061

Prof. Vernon F. Cormier
Department of Geology & Geophysics
U-45, Room 207
University of Connecticut
Storrs, CT 06268

Prof. Steven Day
Department of Geological Sciences
San Diego State University
San Diego, CA 92182

Marvin Denny
U.S. Department of Energy
Office of Arms Control
Washington, DC 20585

Dr. Zoltan Der
ENSCO, Inc.
5400 Port Royal Road
Springfield, VA 22151-2388

Prof. Adam Dziewonski
Hoffman Laboratory, Harvard University
Dept. of Earth Atmos. & Planetary Sciences
20 Oxford Street
Cambridge, MA 02138

Prof. John Ebel
Department of Geology & Geophysics
Boston College
Chestnut Hill, MA 02167

Eric Fielding
SNEE Hall
INSTOC
Cornell University
Ithaca, NY 14853

Dr. Mark D. Fisk
Mission Research Corporation
735 State Street
P.O. Drawer 719
Santa Barbara, CA 93102

Prof Stanley Flatte
Applied Sciences Building
University of California, Santa Cruz
Santa Cruz, CA 95064

Dr. John Foley
NER-Geo Sciences
1100 Crown Colony Drive
Quincy, MA 02169

Prof. Donald Forsyth
Department of Geological Sciences
Brown University
Providence, RI 02912

Dr. Art Frankel
U.S. Geological Survey
922 National Center
Reston, VA 22092

Dr. Cliff Frolich
Institute of Geophysics
8701 North Mopac
Austin, TX 78759

Dr. Holly Given
IGPP, A-025
Scripps Institute of Oceanography
University of California, San Diego
La Jolla, CA 92093

Dr. Jeffrey W. Given
SAIC
10260 Campus Point Drive
San Diego, CA 92121

Dr. Dale Glover
Defense Intelligence Agency
ATTN: ODT-1B
Washington, DC 20301

Dr. Indra Gupta
Teledyne Geotech
314 Montgomery Street
Alexanderia, VA 22314

Dan N. Hagedon
Pacific Northwest Laboratories
Battelle Boulevard
Richland, WA 99352

Dr. James Hannon
Lawrence Livermore National Laboratory
P.O. Box 808
L-205
Livermore, CA 94550

Dr. Roger Hansen
HQ AFTAC/TTR
Patrick AFB, FL 32925-6001

Prof. David G. Harkrider
Seismological Laboratory
Division of Geological & Planetary Sciences
California Institute of Technology
Pasadena, CA 91125

Prof. Danny Harvey
CIRES
University of Colorado
Boulder, CO 80309

Prof. Donald V. Helmberger
Seismological Laboratory
Division of Geological & Planetary Sciences
California Institute of Technology
Pasadena, CA 91125

Prof. Eugene Herrin
Institute for the Study of Earth and Man
Geophysical Laboratory
Southern Methodist University
Dallas, TX 75275

Prof. Robert B. Herrmann
Department of Earth & Atmospheric Sciences
St. Louis University
St. Louis, MO 63156

Prof. Lane R. Johnson
Seismographic Station
University of California
Berkeley, CA 94720

Prof. Thomas H. Jordan
Department of Earth, Atmospheric &
Planetary Sciences
Massachusetts Institute of Technology
Cambridge, MA 02139

Prof. Alan Kafka
Department of Geology & Geophysics
Boston College
Chestnut Hill, MA 02167

Robert C. Kemerait
ENSCO, Inc.
445 Pineda Court
Melbourne, FL 32940

Dr. Karl Koch
Institute for the Study of Earth and Man
Geophysical Laboratory
Southern Methodist University
Dallas, Tx 75275

Dr. Max Koontz
U.S. Dept. of Energy/DP 5
Forrestal Building
1000 Independence Avenue
Washington, DC 20585

Dr. Richard LaCoss
MIT Lincoln Laboratory, M-200B
P.O. Box 73
Lexington, MA 02173-0073

Dr. Fred K. Lamb
University of Illinois at Urbana-Champaign
Department of Physics
1110 West Green Street
Urbana, IL 61801

Prof. Charles A. Langston
Geosciences Department
403 Deike Building
The Pennsylvania State University
University Park, PA 16802

Jim Lawson, Chief Geophysicist
Oklahoma Geological Survey
Oklahoma Geophysical Observatory
P.O. Box 8
Leonard, OK 74043-0008

Prof. Thorne Lay
Institute of Tectonics
Earth Science Board
University of California, Santa Cruz
Santa Cruz, CA 95064

Dr. William Leith
U.S. Geological Survey
Mail Stop 928
Reston, VA 22092

Mr. James F. Lewkowicz
Phillips Laboratory/GPEH
Hanscom AFB, MA 01731-5000(2 copies)

Mr. Alfred Lieberman
ACDA/VI-OA State Department Building
Room 5726
320-21st Street, NW
Washington, DC 20451

Prof. L. Timothy Long
School of Geophysical Sciences
Georgia Institute of Technology
Atlanta, GA 30332

Dr. Randolph Martin, III
New England Research, Inc.
76 Olcott Drive
White River Junction, VT 05001

Dr. Robert Masse
Denver Federal Building
Box 25046, Mail Stop 967
Denver, CO 80225

Dr. Gary McCartor
Department of Physics
Southern Methodist University
Dallas, TX 75275

Prof. Thomas V. McEvilly
Seismographic Station
University of California
Berkeley, CA 94720

Dr. Art McGarr
U.S. Geological Survey
Mail Stop 977
U.S. Geological Survey
Menlo Park, CA 94025

Dr. Keith L. McLaughlin
S-CUBED
A Division of Maxwell Laboratory
P.O. Box 1620
La Jolla, CA 92038-1620

Stephen Miller & Dr. Alexander Florence
SRI International
333 Ravenswood Avenue
Box AF 116
Menlo Park, CA 94025-3493

Prof. Bernard Minster
IGPP, A-025
Scripps Institute of Oceanography
University of California, San Diego
La Jolla, CA 92093

Prof. Brian J. Mitchell
Department of Earth & Atmospheric Sciences
St. Louis University
St. Louis, MO 63156

Mr. Jack Murphy
S-CUBED
A Division of Maxwell Laboratory
11800 Sunrise Valley Drive, Suite 1212
Reston, VA 22091 (2 Copies)

Dr. Keith K. Nakanishi
Lawrence Livermore National Laboratory
L-025
P.O. Box 808
Livermore, CA 94550

Dr. Carl Newton
Los Alamos National Laboratory
P.O. Box 1663
Mail Stop C335, Group ESS-3
Los Alamos, NM 87545

Dr. Bao Nguyen
HQ AFTAC/TTR
Patrick AFB, FL 32925-6001

Prof. John A. Orcutt
IGPP, A-025
Scripps Institute of Oceanography
University of California, San Diego
La Jolla, CA 92093

Prof. Jeffrey Park
Kline Geology Laboratory
P.O. Box 6666
New Haven, CT 06511-8130

Dr. Howard Patton
Lawrence Livermore National Laboratory
L-025
P.O. Box 808
Livermore, CA 94550

Dr. Frank Pilotte
HQ AFTAC/TT
Patrick AFB, FL 32925-6001

Dr. Jay J. Pulli
Radix Systems, Inc.
2 Taft Court, Suite 203
Rockville, MD 20850

Dr. Robert Reinke
ATTN: FCTVTD
Field Command
Defense Nuclear Agency
Kirtland AFB, NM 87115

Prof. Paul G. Richards
Lamont-Doherty Geological Observatory
of Columbia University
Palisades, NY 10964

Mr. Wilmer Rivers
Teledyne Geotech
314 Montgomery Street
Alexandria, VA 22314

Dr. George Rothe
HQ AFTAC/TTR
Patrick AFB, FL 32925-6001

Dr. Alan S. Ryall, Jr.
DARPA/NMRO
3701 North Fairfax Drive
Arlington, VA 22209-1714

Dr. Richard Sailor
TASC, Inc.
55 Walkers Brook Drive
Reading, MA 01867

Prof. Charles G. Sammis
Center for Earth Sciences
University of Southern California
University Park
Los Angeles, CA 90089-0741

Prof. Christopher H. Scholz
Lamont-Doherty Geological Observatory
of Columbia University
Palisades, NY 10964

Dr. Susan Schwartz
Institute of Tectonics
1156 High Street
Santa Cruz, CA 95064

Secretary of the Air Force
(SAFRD)
Washington, DC 20330

Office of the Secretary of Defense
DDR&E
Washington, DC 20330

Thomas J. Sereno, Jr.
Science Application Int'l Corp.
10260 Campus Point Drive
San Diego, CA 92121

Dr. Michael Shore
Defense Nuclear Agency/SPSS
6801 Telegraph Road
Alexandria, VA 22310

Dr. Robert Shumway
University of California Davis
Division of Statistics
Davis, CA 95616

Dr. Matthew Sibol
Virginia Tech
Seismological Observatory
4044 Derring Hall
Blacksburg, VA 24061-0420

Prof. David G. Simpson
IRIS, Inc.
1616 North Fort Myer Drive
Suite 1440
Arlington, VA 22209

Donald L. Springer
Lawrence Livermore National Laboratory
L-025
P.O. Box 808
Livermore, CA 94550

Dr. Jeffrey Stevens
S-CUBED
A Division of Maxwell Laboratory
P.O. Box 1620
La Jolla, CA 92038-1620

Lt. Col. Jim Stobie
ATTN: AFOSR/NL
Bolling AFB
Washington, DC 20332-6448

Prof. Brian Stump
Institute for the Study of Earth & Man
Geophysical Laboratory
Southern Methodist University
Dallas, TX 75275

Prof. Jeremiah Sullivan
University of Illinois at Urbana-Champaign
Department of Physics
1110 West Green Street
Urbana, IL 61801

Prof. L. Sykes
Lamont-Doherty Geological Observatory
of Columbia University
Palisades, NY 10964

Dr. David Taylor
ENSCO, Inc.
445 Pineda Court
Melbourne, FL 32940

Dr. Steven R. Taylor
Los Alamos National Laboratory
P.O. Box 1663
Mail Stop C335
Los Alamos, NM 87545

Prof. Clifford Thurber
University of Wisconsin-Madison
Department of Geology & Geophysics
1215 West Dayton Street
Madison, WS 53706

Prof. M. Nafi Toksoz
Earth Resources Lab
Massachusetts Institute of Technology
42 Carleton Street
Cambridge, MA 02142

Dr. Larry Turnbull
CIA-OSWR/NED
Washington, DC 20505

Dr. Gregory van der Vink
IRIS, Inc.
1616 North Fort Myer Drive
Suite 1050
Arlington, VA 22209

Dr. Karl Veith
EG&G
5211 Auth Road
Suite 240
Suitland, MD 20746

Prof. Terry C. Wallace
Department of Geosciences
Building #77
University of Arizona
Tuscon, AZ 85721

Dr. Thomas Weaver
Los Alamos National Laboratory
P.O. Box 1663
Mail Stop C335
Los Alamos, NM 87545

Dr. William Wortman
Mission Research Corporation
8560 Cinderbed Road
Suite 700
Newington, VA 22122

Prof. Francis T. Wu
Department of Geological Sciences
State University of New York
at Binghamton
Vestal, NY 13901

AFTAC/CA
(STINFO)
Patrick AFB, FL 32925-6001

DARPA/PM
3701 North Fairfax Drive
Arlington, VA 22203-1714

DARPA/RMO/RETRIEVAL
3701 North Fairfax Drive
Arlington, VA 22203-1714

DARPA/RMO/SECURITY OFFICE
3701 North Fairfax Drive
Arlington, VA 22203-1714

HQ DNA
ATTN: Technical Library
Washington, DC 20305

Defense Intelligence Agency
Directorate for Scientific & Technical Intelligence
ATTN: DTIB
Washington, DC 20340-6158

Defense Technical Information Center
Cameron Station
Alexandria, VA 22314 (2 Copies)

TACTEC
Battelle Memorial Institute
505 King Avenue
Columbus, OH 43201 (Final Report)

Phillips Laboratory
ATTN: XPG
Hanscom AFB, MA 01731-5000

Phillips Laboratory
ATTN: GPE
Hanscom AFB, MA 01731-5000

Phillips Laboratory
ATTN: TSML
Hanscom AFB, MA 01731-5000

Phillips Laboratory
ATTN: SUL
Kirtland, NM 87117 (2 copies)

Dr. Michel Bouchon
I.R.I.G.M.-B.P. 68
38402 St. Martin D'Heres
Cedex, FRANCE

Dr. Michel Campillo
Observatoire de Grenoble
I.R.I.G.M.-B.P. 53
38041 Grenoble, FRANCE

Dr. Kin Yip Chun
Geophysics Division
Physics Department
University of Toronto
Ontario, CANADA

Prof. Hans-Peter Harjes
Institute for Geophysic
Ruhr University/Bochum
P.O. Box 102148
4630 Bochum 1, GERMANY

Prof. Eystein Husebye
NTNF/NORSAR
P.O. Box 51
N-2007 Kjeller, NORWAY

David Jepsen
Acting Head, Nuclear Monitoring Section
Bureau of Mineral Resources
Geology and Geophysics
G.P.O. Box 378, Canberra, AUSTRALIA

Ms. Eva Johannisson
Senior Research Officer
FOA
S-172 90 Sundbyberg, SWEDEN

Dr. Peter Marshall
Procurement Executive
Ministry of Defense
Blacknest, Brimpton
Reading FG7-FRS, UNITED KINGDOM

Dr. Bernard Massinon, Dr. Pierre Mechler
Societe Radiomana
27 rue Claude Bernard
75005 Paris, FRANCE (2 Copies)

Dr. Svein Mykkeltveit
NTNT/NORSAR
P.O. Box 51
N-2007 Kjeller, NORWAY (3 Copies)

Prof. Keith Priestley
University of Cambridge
Bullard Labs, Dept. of Earth Sciences
Madingley Rise, Madingley Road
Cambridge CB3 OEZ, ENGLAND

Dr. Jorg Schlittenhardt
Federal Institute for Geosciences & Nat'l Res.
Postfach 510153
D-3000 Hannover 51, GERMANY

Dr. Johannes Schweitzer
Institute of Geophysics
Ruhr University/Bochum
P.O. Box 1102148
4360 Bochum 1, GERMANY

Trust & Verify
VERTIC
8 John Adam Street
LONDON WC2N 6EZ, ENGLAND